The nature of the intermolecular interaction in $(H_2X)_2$ (X = O, S, Se)

Alberto Fernández-Alarcón[a,b], José Manuel Guevara-Vela[a], José Luis Casals-Sainz[b], Evelio Francisco[b], Aurora Costales[b], Ángel Martín Pendás[b,*], Tomás Rocha-Rinza[a,*]

[a] *Institute of Chemistry, National Autonomous University of Mexico, Circuito Exterior, Ciudad Universitaria, Delegación Coyoacán C.P. 04510, Mexico City, Mexico.*
[b] *Department of Analytical and Physical Chemistry, University of Oviedo, E-33006, Oviedo, Spain.*

Abstract

Hydrogen Bonds (HBs) are crucial non-covalent interactions in chemistry. Recently, the occurrence of an HB in $(H_2S)_2$ has been reported (Arunan *et al.*, *Angew. Chem. Int. Ed.* **2018**, *57*, 15199.), challenging the textbook view of H_2S dimers as mere van der Waals clusters. We herein try to shed light on the nature of the intermolecular interactions in the H_2O, H_2S, and H_2Se dimers via correlated electronic structure calculations, Symmetry Adapted Perturbation Theory (SAPT) and Quantum Chemical Topology (QCT). Although $(H_2S)_2$ and $(H_2Se)_2$ meet some of the criteria for the occurrence of an HB, potential energy curves as well as SAPT and QCT analyses indicate that the nature of the interaction in $(H_2O)_2$ is substantially different (e.g. more anisotropic) from that in $(H_2S)_2$ and $(H_2Se)_2$. QCT reveal that the HB in $(H_2O)_2$ includes substantial covalent, dispersion and electrostatic contributions, while the last-mentioned component plays only a minor role in $(H_2S)_2$ and $(H_2Se)_2$. The major contributions to the interactions of the dimers of H_2S and H_2Se are covalency and dispersion as revealed by the exchange-correlation components of QCT energy partitions. The picture yielded by SAPT is somewhat different but compatible with that offered by QCT. Overall, our results indicate that neither $(H_2S)_2$ nor $(H_2Se)_2$ are hydrogen-bonded systems, showing how the nature of intermolecular contacts involving hydrogen atoms evolve in a group down the periodic table.

*To whom correspondence should be addressed: ampendas@uniovi.es, trocha@iquimica.unam.mx

Keywords:
Hydrogen bond, Interacting Quantum Atoms, Quantum Theory of Atoms in Molecules, Anisotropy, Ionic and covalent contributions.

Introduction

Hydrogen bonds (HBs) are interactions among closed-shell species of prominent relevance in supramolecular chemistry, crystal engineering, molecular biology and material science [1–4]. Among the phenomena that depend on HBs we may enumerate the extraordinary properties of water, the pairing mechanism between DNA nucleobases, or the formation of acid rain [5–7], to name just a few. The relevance of H-bond has been addressed by Pairas and Tsoungas [8] in which the hydrogen atom acts as a bridge between two moieties in a system in different circumstances. From its original description as a relatively weak hydrogen-mediated union between valence-saturated molecules [9], one hundred years ago, the concept of an HB has evolved as a result of new developments in the understanding of non-covalent interactions. At the time of writing, the IUPAC states that [10]:

> *"The hydrogen bond is an attractive interaction between a hydrogen atom from a molecule or a molecular fragment X-H in which X is more electronegative than H, and an atom or a group of atoms in the same or a different molecule, in which there is evidence of bond formation."*

This definition includes a large variety of interactions, such as the partial donation of a hydrogen atom to a π system [11], the interaction of a strong Lewis basis with acetylenic hydrogens [12], or many CH···O=C contacts [6]. Indeed, it is difficult to establish clear boundaries among the different interactions referred as hydrogen bonds [13]. In this regard, the H_2S dimer was recently characterised as a hydrogen-bonded cluster through microwave spectroscopy and electronic structure calculations [14]. The description of the $H_2S\cdots H_2S$ interaction as an HB is in contrast with the traditional consideration of $(H_2S)_2$ as a mere van der Waals cluster. This last view is supported by studies of hydrogen sulphide at low pressures [15]. Loveday *et al.* [15] wrote in this

regard that *"the ambient pressure structures of hydrogen sulphide do not appear to be influenced by H bonding at all"* and *"At ambient pressure the hydrogen bonding in hydrogen sulphide appears to be absent or very weak"*. Certainly, the solid phases of H_2S at low pressures (phases I, II and III in Figure 1 of reference [15]) are not hydrogen-bonded [15, 16]. We also point out that there are solid phases of H_2S which present H-bonding at high pressures (specifically phase I$'$ considered in reference [15]). Pressure can indeed alter chemical bonding. For example, it can transform metals into insulators (*e.g.*, the transparent phase of Li [17]), or it can activate very strong chemical bonds (*e.g.*, CO or N_2 polymerisation [18–20]). H-bonding can also be affected by pressure [15]. Nevertheless, the fact that H_2S units might form hydrogen bonds at high pressures does not provide any information about the interaction in the gas phase dimer and how we should classify it.

Given the paramount importance of hydrogen bonds, the critical assessment of these opposite views in the H_2S dimer is particularly relevant, constituting the main aim of this work. The consideration of this case where the occurrence of an HB raises controversy is also intended to contribute to a better appreciation of the variability and complexity of hydrogen bonds. More in detail, we have thoroughly characterised the intermolecular interactions in three hydrogen chalcogenide dimers, i.e., $(H_2O)_2$, $(H_2S)_2$ and $(H_2Se)_2$, via correlated electronic structure calculations and wave function analyses, with a special emphasis in state-of-the-art real space approaches defined in Quantum Chemical Topology (QCT) [21, 22]. The examination of vector and scalar fields derived from computed wave functions via QCT offers new perspectives and insights in the characterisation of different kinds of interactions in chemistry. These methods have been previously used to study a wide range of systems and processes, e.g. lone pair- and anion-arene interactions [23, 24], the partitioning of dynamic correlation [25, 26], and the nature of halogen bonding [27, 28], beryllium bonds [29], or aurophilic contacts in coordination compounds [30, 31]. Regarding HBs, QCT methodologies have been successfully employed in the study of several systems and topics such as (i) the properties of intramolecular HBs [32, 33], (ii) the interplay among π skeletons and hydrogen bonds [34, 35], (iii) the origin of HB cooperative and anticooperative effects [36, 37] and (iv) the origin of hypso- and bathocromism induced by HBs. [38, 39] The

strong record of QCT tackling difficult or controversial problems encouraged us to use its methods to investigate the character of the intermolecular interactions present in the above mentioned dimers.

Altogether, the comparison of $(H_2O)_2$, $(H_2S)_2$ and $(H_2Se)_2$ provides a clear description of the intermolecular interactions in each of these systems. Our analyses point to close similarities between $(H_2S)_2$ and $(H_2Se)_2$ in contrast with the H-bonded $(H_2O)_2$, particularly the anisotropic character and the balance between the covalent and electrostatic contributions to the intermolecular interaction. These results raise the question whether $(H_2S)_2$ should be truly regarded as a hydrogen-bonded cluster [14], and they provide important clues about how the nature of the intermolecular contacts change with the electronegativity of the atoms involved in the interaction.

Theoretical framework

Briefly, QCT embraces a set of methods that allow the study of the electron distribution in real (as opposed to orbital) space, and it started with the Quantum Theory of Atoms In Molecules (QTAIM) [40], proposed by Bader and coworkers. The QTAIM is based on a topological analysis of the electron density scalar field, $\rho(\mathbf{r})$, which induces a partition of the real space into disjoint regions, or basins, that are identified with the atoms of chemistry [41]. These basins are proper quantum subsystems for which it is possible to calculate expectation values of quantum-mechanical observables, i.e., atomic properties [42].

The Interacting Quantum Atoms (IQA) approach is built on top of the QTAIM partition of real space, defining a division of the total electronic energy of a system into intra- (or net-) and inter-atomic terms [43], $E_{\text{elec}} = \sum_A E^A_{\text{net}} + \frac{1}{2}\sum_{A\neq B} E^{AB}_{\text{int}}$. This partition is fully orbital-invariant, depending only on the wave function of the examined system. The IQA interatomic interaction energy E^{AB}_{int} can be further partitioned into electrostatic (or classical) and quantum-mechanical (or exchange-correlation) contributions, $E^{AB}_{\text{int}} = E^{AB}_{\text{class}} + E^{AB}_{\text{xc}}$. The former measures ionicity and the latter covalency plus dispersion in the case of intermolecular interactions [44]. Covalent and dispersion contributions can be approximately separated by splitting E^{AB}_{xc} into exchange

and correlation components $E_{\mathrm{xc}}^{AB} = E_{\mathrm{x}}^{AB} + E_{\mathrm{corr}}^{AB}$. [26] Nevertheless, this separation is seldom performed. The effects of the correlated motion of electrons at long-range between two atoms that interact can be described in standard perturbations theory, like dispersion corrections to the interaction energy. It is traditionally accepted that the dispersion energy is a stabilising component of the total interaction energy, as well as the exchange correlation term in short-range interactions. Nevertheless, at intermediate range it is far from clear what dispersion is and how it can be disentangled from other contributions. This applies to all energy decomposition analyses including IQA. Casals-Sainz et al. in reference [45] showed that all terms related to the dispersion energy at long-range modify the correlation contributions ones at short distance. It is to be noticed that there is not an unambiguous way to separate exchange-correlation components from the dispersion ones in a short-range regime. The ability to calculate the interaction energy among pairs of atoms (or of arbitrary sets of those atoms, i.e., fragments) in a molecular system E_{int}^{AB}, and to further separate it into chemically appealing terms makes IQA particularly useful in the study of molecular clusters.

In addition to the electron or pair densities, there are other scalar fields whose topological analyses have provided valuable insights about chemical bonding [28, 46, 47]. One of such fields is the Electron Localisation Function (ELF), whose inspection leads to the identification of important concepts in covalent bonding such as core, lone, and bonding electron pairs. The ELF is a measure of how fast the probability of finding a second electron with the same spin as that of a reference one decays in space. It was first introduced by Becke and Edgecombe [48] for Hartree-Fock state vectors and later generalised by Savin and coworkers to density functional theory [49]. The ELF has been extensively used in the study of chemical interactions driven by the interplay of electron pairs [28, 35, 50].

Another relevant method of wave function analysis in the realm of QCT is that of the Non-Covalent Interactions (NCI)-index developed by Johnson et al. [51] The NCI-index is a kinetic energy-based descriptor that uses the reduced density gradient, $s(\mathbf{r}) = |\nabla\rho(\mathbf{r})|/\rho(\mathbf{r})^{4/3}$, and the second eigenvalue of the Hessian of the electron density, λ_2, to characterise non-covalent interactions. The isosurfaces of $s(\mathbf{r})$, coloured by the value of $\mathrm{sgn}(\lambda_2)\rho(\mathbf{r})$, have been shown to be

very useful to uncover the nature of several non-covalent contacts such as dispersion forces [52]. The NCI-index has become an important tool in the study of weak interactions regardless of their association to bond paths in the QTAIM [33].

Besides the wave function analyses discussed above, we considered the Symmetry Adapted Perturbation Theory (SAPT) [53] to investigate the nature of the addressed dimers. The SAPT approach allows us to compute the non-covalent interaction energy between two species without the explicit computation of the properties of the dimer. We start by considering the polarisation approximation, which is the simplest perturbation theory approach for the description of intermolecular interactions A···B. This method starts from the equation,

$$\left(\widehat{H}_0 + \widehat{V}\right)|\Psi_{\rm AB}\rangle = E_{\rm AB}|\Psi_{\rm AB}\rangle, \tag{1}$$

wherein $E_{\rm AB}$ and $|\Psi_{\rm AB}\rangle$ are the ground state energy and wave function of the composite system A···B. The zero-order Hamiltonian, $\widehat{H}_0 = \widehat{H}^{\rm A} + \widehat{H}^{\rm B}$, is the sum of the electronic Hamiltonians of monomers A and B, while $\widehat{V}$ is the Hamiltonian of interaction between these species,

$$\widehat{V} = \sum_{e_a \in {\rm A}} \sum_{e_b \in {\rm B}} \frac{e_a e_b}{r_{ab}}. \tag{2}$$

Standard perturbation theory leads to the definition of electrostatic, as the first order energy in the perturbation theory expansion,

$$E^{(1)}_{\rm elst}({\rm AB}) = \langle 00|\widehat{V}|\,00\rangle, \tag{3}$$

wherein $|00\rangle$ is the ground state composite wave function in the set $\{|mn\rangle\}$ in which, m and n go over all the electronic states of molecules A and B respectively. The component $E_{\rm elst}$ equals the Coulombic interaction of the unperturbed charge densities of A and B. The second order energy is divided in induction and dispersion contributions,

$$E^{(2)}_{\rm ind}({\rm A}) = -\sum_{m\neq 0} \frac{\langle 00|\widehat{V}|m0\rangle\langle m0|\widehat{V}|00\rangle}{W^{\rm A}_m - W^{\rm A}_0}, \tag{4}$$

$$E^{(2)}_{\rm ind}({\rm B}) = -\sum_{n\neq 0} \frac{\langle 00|\widehat{V}|n0\rangle\langle n0|\widehat{V}|00\rangle}{W^{\rm B}_n - W^{\rm B}_0}, \tag{5}$$

$$E^{(2)}_{\rm disp}({\rm AB}) = -\sum_{n\neq 0,\, m\neq 0} \frac{\langle 00|\widehat{V}|mn\rangle\langle mn|\widehat{V}|00\rangle}{W^{\rm A}_m + W^{\rm B}_n - W^{\rm A}_0 - W^{\rm B}_0}, \tag{6}$$

in which $W^{\rm A}_m$ and $W^{\rm B}_n$ represent the corresponding energy eigenvalues of the m-th and n-th electronic states of A and B respectively. $E^{(2)}_{\rm ind}({\rm A})$ denotes the interaction energy due to the distortion of the electronic charge density and nuclear arrangement of A by virtue of the electrical potential imposed by the unperturbed charge density of B, and vice versa for $E^{(2)}_{\rm ind}({\rm B})$. On the other hand, $E^{(2)}_{\rm disp}({\rm AB})$ is related to the correlation of the motion of the electrons between the two molecules.

Expressions (3)–(6) do not take into account the proper Pauli antisymmetry of $|\Psi_{\rm AB}\rangle$ for the exchange of electrons between molecules A and B. After tackling this problem, one obtains that the formation energy $E_{\rm form}({\rm AB})$ of the cluster is given by a sum of physically distinct contributions,

$$E_{\rm form}({\rm AB}) = E^{(1)}_{\rm pol} + E^{(1)}_{\rm exch} + E^{(2)}_{\rm pol} + E^{(2)}_{\rm exch} + \ldots = \sum_n \left(E^{(n)}_{\rm pol} + E^{(n)}_{\rm exch}\right), \tag{7}$$

wherein $E^{(n)}_{\rm exch}$ are the correction of order n due to the exchange of electrons between A and B. Because neither of the electronic problems for molecules A and B is solved in practice, a three-parameter perturbation theory is applied in which $\widehat{H}^0$, is the sum of the Fock operators for A and B, $\widehat{H}^0 = \widehat{F}^{\rm A} + \widehat{F}^{\rm B}$, and the perturbation is given by the sum of $\widehat{V}$ in equation (2) along with $\widehat{\Phi}_{\rm A}$ and $\widehat{\Phi}_{\rm B}$, the fluctuation potentials for molecules A and B. Hence, the full electronic Hamiltonian becomes

$$\widehat{H} = \widehat{H}^0 + \left(\zeta\widehat{V} + \lambda_{\rm A}\widehat{\Phi}_{\rm A} + \lambda_{\rm B}\widehat{\Phi}_{\rm B}\right), \tag{8}$$

and hence, the formation energy of the complex A$\cdots$B reads

$$E_{\rm form}({\rm AB}) = \sum_{n=0}^{\infty}\sum_{i=0}^{\infty}\sum_{j=0}^{\infty}\left(E^{(nij)}_{\rm pol} + E^{nij}_{\rm exch}\right), \tag{9}$$

in which $E_{\mathrm{pol}}^{(nij)}$ are of n-th, i-th and j-th order in $\widehat{V}$, $\widehat{\Phi}_{\mathrm{A}}$ and $\widehat{\Phi}_{\mathrm{B}}$. We emphasise that the SAPT theoretical framework was developed to study NCIs and it should not be intended to examine the covalent component of intermolecular contacts. Nevertheless, we decided to include a SAPT energy decomposition analysis to complement the QCT results, since there are many studies in which SAPT is used to understand and characterise intermolecular forces [53].

Results and discussion

One of the principal arguments put forward by Arunan and coworkers to describe the intermolecular bonding in $(H_2S)_2$ as a hydrogen bond is built on its geometric structure [14]. We agree with the experimental evidence that these authors present and with their interpretation of the nature of the corresponding intermolecular interactions based on such structure. Figure 1 shows that the equilibrium configuration of $(H_2S)_2$ is indeed similar to that of the water dimer. Moreover, the distances H···O/S/Se are smaller than the corresponding sums of the van der Waals radii ($\sum r_{\mathrm{vdW}}$) in the examined systems. Nonetheless, the distance between the H3 (see Figure 1 for the atoms numbering) and S1 atoms is 0.77 Å larger than the O1···H3 distance in the water dimer, although the van der Waals radius of S is only 0.28 Å longer than that of O. A more stringent criterion for the occurrence of an H-bond concerns the comparison of the distances O/S/Se···O/S/Se with $\sum r_{\mathrm{vdW}}$. Only the O···O distance in $(H_2O)_2$ is smaller than $\sum r_{\mathrm{vDW}}$ as compared with S···S and Se···Se in $(H_2S)_2$ and $(H_2Se)_2$. Goswami and Arunan [54] indicated that the test for the occurrence of hydrogen bonds based on O/S/Se···H and O/S/Se···O/S/Se distances have been criticised as too tolerant and too rigid respectively. There is a marked difference in the dihedral angle generated by the planes of the molecules in the two clusters. While for the water dimer, this angle is about 125°, for the hydrogen sulphide dimer it is around 135°. Our analyses below show that this difference is related to the distinct anisotropic character of the purported HB interactions. Figure 1 also indicates that the structures of the hydrogen sulphide and selenide dimers are practically identical. Quantum chemical topology analyses show that the similarities between $(H_2S)_2$ and $(H_2Se)_2$ go indeed beyond their structures and that the bonding situation of these two clusters is nearly equivalent.

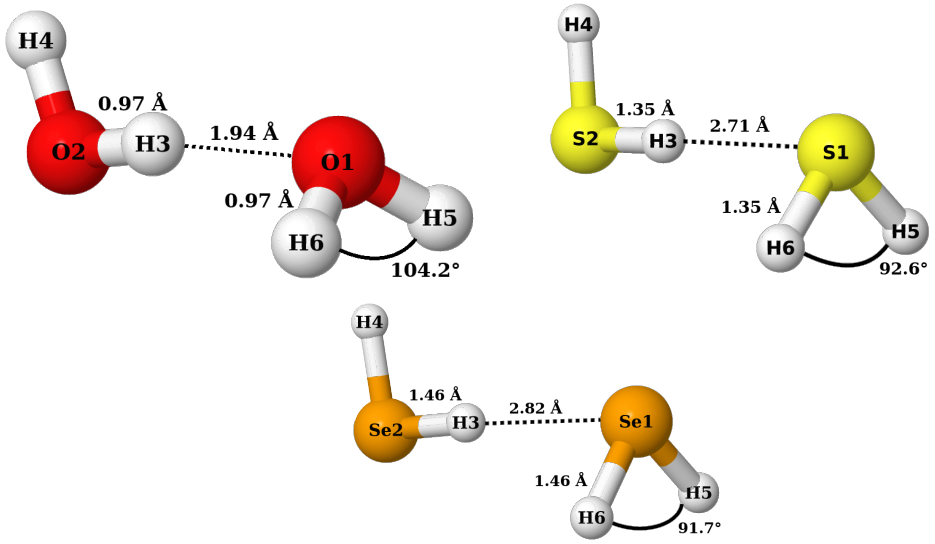

Figure 1: Structure and some geometric parameters for the $(H_2O)_2$, $(H_2S)_2$ and $(H_2Se)_2$ clusters computed with the MP2/aug-cc-pVDZ approximation.

Now, we consider the global energetics of cluster formation, focusing on the existence/absence of cooperativity and directionality effects, and then we move on to the local description of chemical bonding uncovered with QCT tools.

Are the intermolecular interactions in $(H_2S)_2$ and $(H_2Se)_2$ enhanced by cooperativity effects?

An HB can modify the formation energy of other HBs. H-bond cooperative effects occur when HBs within a molecular cluster strengthen each other. On the other hand, HBs might also weaken due to other HBs. This effect is known as HB anticooperativity. A relatively simple way to measure cooperative (or anticooperative) effects in hydrogen-bonded clusters is by comparing (i) the energy associated with the sequential formation of H-bonds,

$$(H_2E)_{n-1} + H_2E \longrightarrow (H_2E)_n \tag{10}$$

ΔE_n, in which E =O, S, Se and (ii) the energy related with the generation of an isolated H-bond, ΔE_2, via,

$$\Delta\Delta E_n = \Delta E_n - \Delta E_2. \tag{11}$$

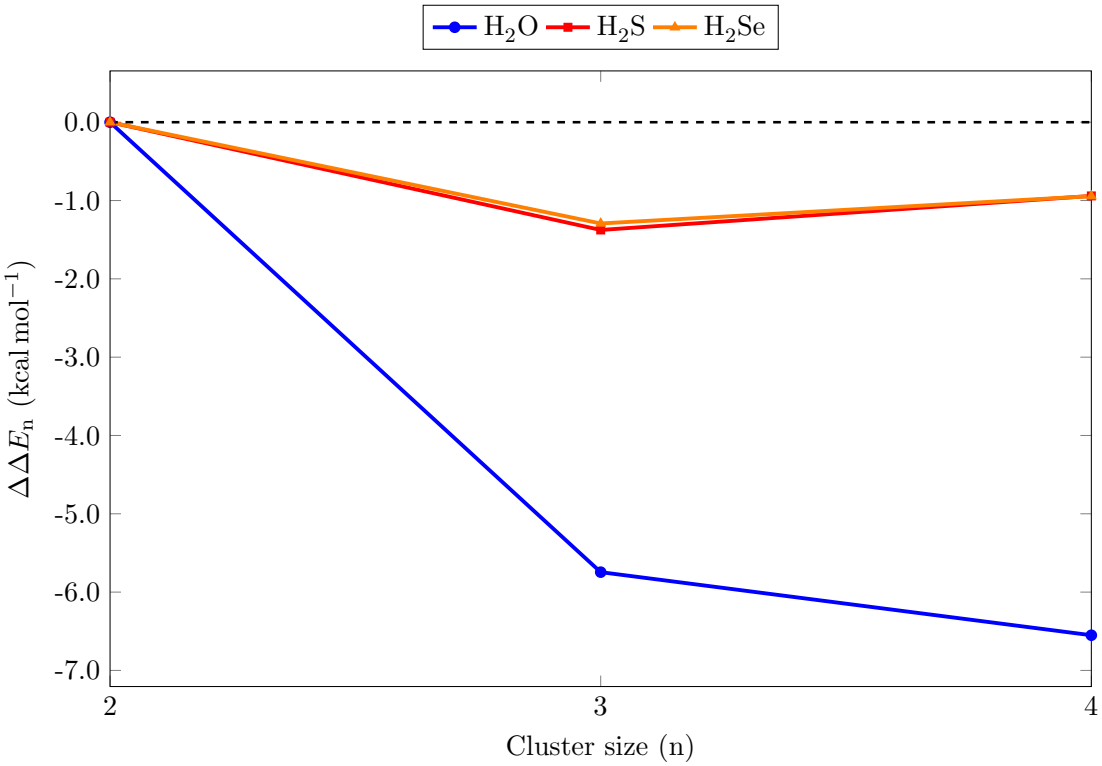

Figure 2: Comparison among the values of $\Delta\Delta E_{\rm n}$ (equation (11)) for the clusters $(H_2E)_n$ with E = O, S, Se and n =2 to 4.

A negative/positive value of $\Delta\Delta E_{\rm n}$ indicates that the addition of an extra molecule to $(H_2E)_{n-1}$ is energetically more/less favourable than the formation of the dimer from the isolated monomers. We have determined the values of $\Delta\Delta E_{\rm n}$ for n = 2 to 4 at the CCSD/aug-cc-pVQZ approximation and show the corresponding results in Figure 2. There is a clear distinction among the magnitude of the $\Delta\Delta E_{\rm n}$ values for the H_2O clusters on one hand, and for those of H_2S and H_2Se on the other. The former are more than five times larger than the latter, indicating considerably non-additive effects in water clusters with respect to those displayed by the sulphur and selenium hydrides. We can observe, however, that the three investigated dimers exhibit cooperative effects, as reflected in the negative values of $\Delta\Delta E_{\rm n}$ for the corresponding trimers and tetramers [55]. This observation of cooperativity represents an indication of H-bonding in the examined systems.

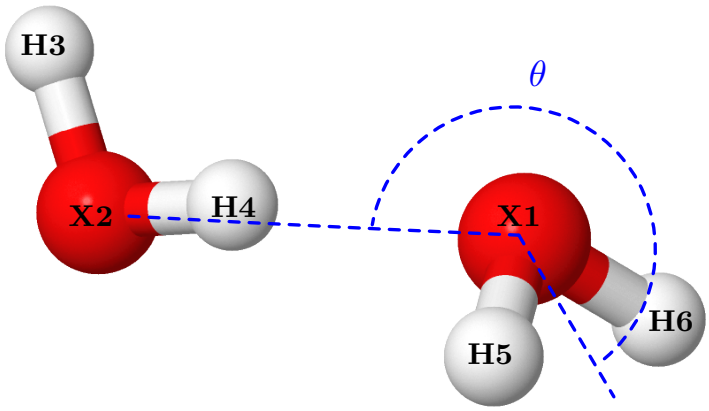

Figure 3: Angle θ formed by the chalcogen atoms of both the hydrogen donor and the hydrogen acceptor molecules, and the midpoint between the hydrogen atoms in the H-acceptor molecule. The figure shows the particular case of the water dimer. This angle is used to plot the potential energy curves of Figure 4.

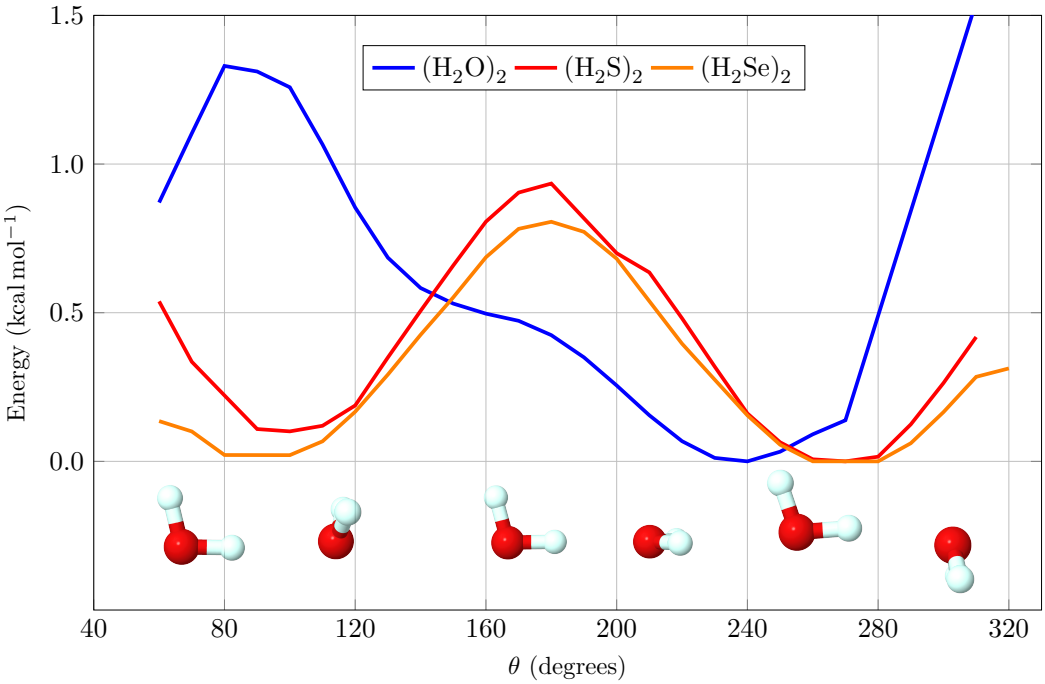

Figure 4: Potential energy curves for the H_2O, H_2S and H_2Se dimers as a function of the angle θ shown in Figure 3. A representation of the first, halfway and final structures is also included. The values are reported in kcal mol^{-1}.

Are the intermolecular interactions in $(H_2S)_2$ and $(H_2Se)_2$ anisotropic?

One important aspect of HBs is their directionality, a key factor to rationalise the structure of ice and liquid water as well as to understand many important molecular recognition processes in biology. Although HB directionality is often considered via the angle X−H···Y, one might examine other geometrical parameters to assess this feature of H-bonds. For example, we computed potential energy curves as a function of the angle θ defined in Figure 3. As one can see in Figure 4, the general form of the potential energy curve for $(H_2O)_2$ is considerably different from those for $(H_2S)_2$ and $(H_2Se)_2$. In the first-mentioned case, the electronic energy is a monotonically decreasing function of θ when $\theta \in [80°, 240°]$. However, for $(H_2S)_2$ and $(H_2Se)_2$, the energy increases with θ, until it reaches a maximum at 180° that is around $1.0\,\mathrm{kcal\,mol^{-1}}$ less stable than the global energetic minimum. As the angle is raised above 180°, the energy decreases until it reaches another local minimum, very similar in energy to the one found at smaller θ angles. The differences found at $\theta \approx 90°$ for $(H_2O)_2$ with respect to $(H_2S)_2$ and $(H_2Se)_2$ indicate that either (i) there are some stabilising elements present in the two-last mentioned clusters that it is absent in the water dimer or (ii) there are destabilising contacts in $(H_2O)_2$ which are missing in $(H_2S)_2$ and $(H_2Se)_2$ in the proximities of this value of θ. In any case these considerations help to rationalise the smaller barrier for torsion for H_2S and H_2Se dimers. Additionally, one might conjecture that the dissimilarities around $\theta \approx 90°$ for $(H_2O)_2$ with respect to $(H_2S)_2$ and $(H_2Se)_2$ are immaterial to discuss the nature of the interaction at $\theta \approx 240°$. We would like to stress three points in this regard. First, this behaviour of $(H_2S)_2$ and $(H_2Se)_2$ observed in the potential energies of Figure 4 is not accordant with additional criteria put forward by IUPAC to consider an interaction as an HB *"Hydrogen bonds show directional preferences and influence packing modes in crystal structures"* [10]. We recall at this point that the crystalline phases of H_2S at low pressures are not H-bonded [15, 16], in sharp contrast with that of ice. Second, the potential energy curve for $(H_2O)_2$ in Figure 4 is fundamentally, *i.e.* topologically, different from that of $(H_2S)_2$ and $(H_2Se)_2$. Thus, the interaction in $(H_2O)_2$ is much more anisotropic than it is in $(H_2S)_2$ or $(H_2Se)_2$, and therefore of a dissimilar nature. Third, H_2Se and H_2S molecules have net dipole moments as isolated species and within the corresponding dimers (Table S118 in

the Esi). Dipole-dipole ($\boldsymbol{\mu\mu}$) interactions are, of course, anisotropic (equation (2) in the Esi). Accordingly, the configurations displayed on the bottom-left and bottom-right parts of Figure 4 have different $\boldsymbol{\mu\mu}$ interaction energies. The $\boldsymbol{\mu\mu}$ contributions for the configurations in the bottom-right part of Figure 4 are 2.2 kcal mol^{-1} and 1.0 kcal mol^{-1} more stable than those in the bottom-left part for $(H_2S)_2$ and $(H_2Se)_2$ respectively. Still, these configurations are nearly isoenergetic as shown in Figure 4. Therefore, there must exist other more relevant contributions than dipole-dipole interactions in these arrangements of $(H_2S)_2$ and $(H_2Se)_2$.

Other studies concerning dimers of third row hydrides indicate that the interaction of dimers of third row hydrides is dispersion. [56] Dispersion energy between two molecules A and B is given in standard perturbation theory by equation (6). The operator $\widehat{V}$ in formula (2) can be represented using the multipole expansion and the Einstein summation convention as,

$$\widehat{V} = Tq^{\mathrm{A}}q^{\mathrm{B}} + T_\alpha\left(q^{\mathrm{A}}\widehat{\boldsymbol{\mu}}^{\mathrm{B}}_\alpha - q^{\mathrm{B}}\widehat{\boldsymbol{\mu}}^{\mathrm{A}}_\alpha\right) - T_{\alpha\beta}\widehat{\boldsymbol{\mu}}^{\mathrm{A}}_\alpha\widehat{\boldsymbol{\mu}}^{\mathrm{B}}_\beta + \ldots \tag{12}$$

in which the Greek letters $\alpha, \beta \ldots$ denote Cartesian coordinates, $T = (4\pi\epsilon_0 R)^{-1}$ with R being the separation between the mass centers of molecules A and B, and

$$T_{\alpha\beta\ldots\nu} = \frac{1}{4\pi\epsilon_0}\nabla_\alpha\nabla_\beta\ldots\nabla_\nu\frac{1}{R}. \tag{13}$$

Finally $q^{\mathrm{X}}, \widehat{\boldsymbol{\mu}}^{\mathrm{X}}, \ldots$ in equation (12) represent the charge, the dipole moment operators of molecule X. The substitution of expression (12) in formula (6) indicates that the dispersion energy is anisotropic in principle. Different workers such as Chałasiński, Szczęśniak and S. Scheiner [57, 58] have considered the anisotropy of van der Waals complexes such as Ar···HF and Ar···H_2O. Nevertheless, the orientation dependence of the intermolecular contacts governed by dispersion is much less marked than that exhibited by hydrogen bonds as observed in (i) the comparison of CH···π interactions with H-bonded systems [59] and in (ii) the potential energy curves of Figure 4.

Yet another possible explanation regarding the general form of the curves presented in Figure 4 involves the interaction of the lone pairs of the chalcogen atoms in the H-acceptor monomers with the proton of the H-donor molecule. Because the presence of a lone pair is a strong requirement

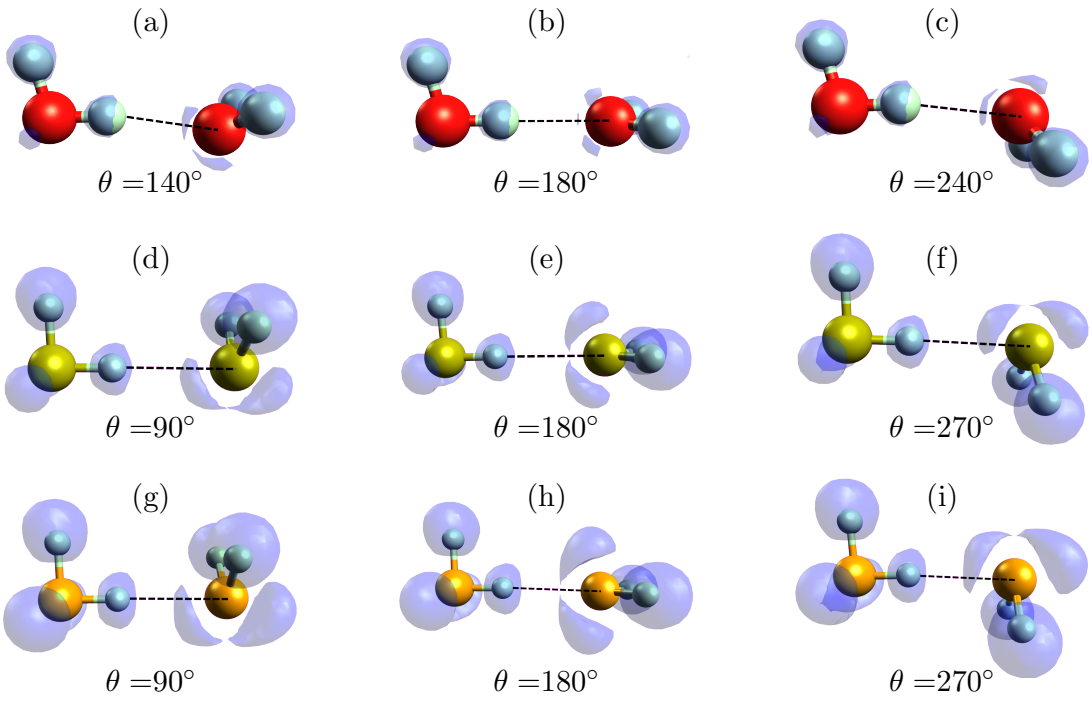

Figure 5: ELF bifurcation analysis [60, 61] for $(H_2O)_2$ (η = 0.9035), $(H_2S)_2$ (η = 0.9245) and $(H_2Se)_2$ (η = 0.8690) systems. The dashed lines connect the intermolecular hydrogen atom and the chalcogen in the H-acceptor molecule.

for the existence of an H-bond [62, 63], we decided to perform the ELF bifurcation analysis for selected points of the examined potential energy curves (Figure 5). For instance, at the equilibrium geometry of $(H_2O)_2$ (Figure 5 (c)) one of the lone pairs in the oxygen atom of the HB acceptor points directly towards the hydrogen bonding atom in the HB donor. Figures 5 (f) and (i) show the ELF isosurfaces for $(H_2S)_2$ and $(H_2Se)_2$ respectively at their equilibrium geometries. In these cases, no lone pair of the sulphur and selenium atoms in the potential hydrogen-acceptor molecule points directly to the hydrogen atom in the intermolecular region, a condition which indicates that $(H_2S)_2$ and $(H_2Se)_2$ do not behave in the same way as other hydrogen-bonded clusters. We also note that the lone pairs in $(H_2O)_2$ is considerably less widespread than it is in $(H_2S)_2$ and $(H_2Se)_2$. This observation is relevant because more localized charge concentrations lead to stronger electrostatic interactions and therefore to a more marked anisotropy. Therefore, the ELF analyses indicate that the larger anisotropic character of the $(H_2O)_2$ curve as compared

occurs in virtue of a molecular property, in similar terms to the $\boldsymbol{\mu\mu}$ interaction discussed above. In other words, the more localized equivalent lone pairs[1] in H_2O result in a more anisotropic interaction in its dimer than it is in their counterparts H_2S and H_2Se. Figures 5 (b), (e) and (h) show the ELF isosurfaces of $(H_2O)_2$, $(H_2S)_2$ and $(H_2Se)_2$, respectively, when $\theta = 180°$. This situation corresponds to the maximum in energy for the potential energy curves of $(H_2S)_2$ and $(H_2Se)_2$. We note that the intermolecular hydrogen atom points directly towards the middle of the lone pairs of the H-acceptor atom when $(H_2S)_2$ and $(H_2Se)_2$ are in this conformation. In the case of $(H_2O)_2$, however, we can observe a remnant of a lone pair pointing towards the proton in the intermolecular region. Finally, Figures 5 (a), (d) and (g) are related with the left part of Figure 4. We point here two critical facts. First, the ELF isosurface of the $(H_2O)_2$ system (Figure 5 (a)) corresponds to the shoulder in the potential energy curve of $(H_2O)_2$ in Figure 4 (θ =140°), where we can observe that a lone pair in the receptor oxygen atom points to the hydrogen atom involved in the HB interaction. Second, the ELF isosurfaces that correspond with the local minimum values in the potential energy curves for $(H_2S)_2$ and $(H_2Se)_2$ (Figures 5 (d) and (g)) indicate that the receptor molecule interacts with the intermolecular hydrogen atom in a very similar way that those presented for the equilibrium geometries (Figures 5 (f) and (i)). The difference between Figures 5(d) and 5(f) (as well as Figures 5(g) and 5(i)) is a vertical flipping of the H-acceptor molecule which do not affect the energetics of the interaction, as observed, in Figure 4. These results are in good agreement with the above discussion of the more significant anisotropic character of the interaction in $(H_2O)_2$ as compared to that in $(H_2S)_2$ and $(H_2Se)_2$.

[1]The point group of H_2O, H_2S and H_2Se is $\mathscr{C}_{2v}$. Because every symmetry transformation in $\mathscr{C}_{2v}$ is its own inverse (i) $\mathscr{C}_{2v}$ is an Abelian group, (ii) all its irreducible representations are unidimensional and (iii) the corresponding characters for an operation in any of these irreducible representation are either $+1$ or -1. Thus, the square of the wave function, and hence of any distribution function, is completely symmetric with respect to any transformation of $\mathscr{C}_{2v}$ and therefore the lone pairs in these systems are necessarily equivalent despite some interpretations of the photoelectron spectroscopy of the water molecule which support the non-equivalence of these lone-pairs.

The hydrogen bond as revealed by the NCI, QTAIM and IQA real space analyses

In order to gain a better understanding of the intermolecular interactions within the dimers addressed herein, we carried out additional real space analyses in accordance with QCT. We used the QTAIM to investigate the chemical bonding scenario in these systems. Specifically, we compared the properties in the Intermolecular Bond Critical Point (IBCP) between the chalcogen atom in the H-acceptor molecule and the hydrogen atom in the intermolecular region. Table 1 shows the Laplacian of the electron density at the IBCP, $\nabla^2\rho(\mathbf{r}_{\mathrm{IBCP}})$, which is small and positive for all cases, a property which characterises the examined interactions as closed-shell contacts, as expected. We can also observe that the electron density at the IBCP ($\rho(\mathbf{r}_{\mathrm{IBCP}})$) for $(H_2O)_2$ is more than twice larger that it is for $(H_2S)_2$ and $(H_2Se)_2$. Ditto for the magnitude of the potential energy density at the $\mathbf{r}_{\mathrm{IBCP}}$. We also point out that $\nabla^2\rho(\mathbf{r}_{\mathrm{IBCP}})$ is significantly larger in $(H_2O)_2$ that in its sulphur and selenium analogues. These values indicate much weaker interactions for $(H_2S)_2$ and $(H_2Se)_2$ with respect to the hydrogen bond in $(H_2O)_2$. Nevertheless, other QTAIM indicators show a more complex picture. The intermolecular delocalisation index, $\mathrm{DI}(H_2X\cdots H_2X)$ presents no clear tendency with respect to the formation energy of the cluster (ΔE_f). The transfer of electron density, defined as the electronic charge donated to the hydrogen-bond donor molecule $\Delta q_{\mathrm{Total}}$, shows that it increases with the size of the chalcogen and it does not correlate with ΔE_f.

Similar results that those yielded by QTAIM are obtained via the NCI-index, which offers a different perspective of intermolecular interactions. Figure 6 shows the NCI isosurfaces for the different examined dimers. Although the isosurfaces of $s(\mathbf{r})$ are similar in shape and size for the three investigated clusters, the NCI-index indicates that the intermolecular interaction in $(H_2O)_2$ is considerably stronger than it is for $(H_2S)_2$ and $(H_2Se)_2$ in correspondence with the electronic structure calculations.

We present now the IQA dissection of the formation energy of the addressed dimers. We recall at this point that the formation energy of a $\mathcal{G}\cdots\mathcal{H}$ molecular cluster, ΔE, can be decomposed as

Table 1: QTAIM parameters that characterise the intermolecular interaction in the studied clusters. The labels correspond with those shown in Figure 1. Atomic units are use throughout except for E_{HB} which is reported in kcal mol^{-1}.

Descriptor	$(H_2O)_2$	$(H_2S)_2$	$(H_2Se)_2$
$\rho(\mathbf{r}_{\mathrm{IBCP}})$	0.026	0.011	0.011
$\nabla^2\rho(\mathbf{r}_{\mathrm{IBCP}})$	0.086	0.028	0.025
$V(\mathbf{r}_{\mathrm{IBCP}})$	−0.019	−0.006	−0.006
$\Delta E_f^{\dagger}$	−5.96	−1.88	−1.88
DI($H_2X\cdots H_2X$)	0.139	0.119	0.135
$\Delta q_{\mathrm{Total}}$	0.017	0.019	0.023

† Computed as indicated in ref. [64]

$$\begin{aligned}\Delta E &= E(\mathcal{G}\cdots\mathcal{H}) - E(\mathcal{G}) - E(\mathcal{H}) \\ &= \Delta E_{\mathrm{def}}^{\mathcal{G}} + \Delta E_{\mathrm{def}}^{\mathcal{H}} + E_{\mathrm{int}}^{\mathcal{G}\cdots\mathcal{H}},\end{aligned} \tag{14}$$

wherein $\Delta E_{\mathrm{def}}^{\mathcal{G}}$ and $\Delta E_{\mathrm{def}}^{\mathcal{H}}$ are the deformation energies of the fragments $\mathcal{G}$ and $\mathcal{H}$ [65] and $E_{\mathrm{int}}^{\mathcal{G}\cdots\mathcal{H}} = \sum_{A\in\mathcal{G}}\sum_{B\in\mathcal{H}} E_{\mathrm{int}}^{AB}$. Figure 7 presents the intermolecular interaction energy components, as well as

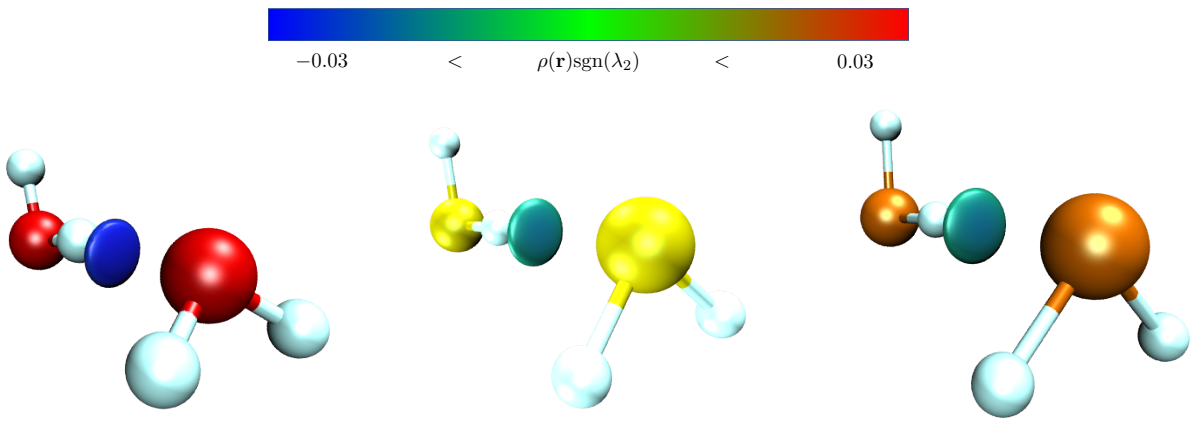

(a) (b) (c)

Figure 6: NCI isosurfaces for (a) $(H_2O)_2$, (b) $(H_2S)_2$ and (c) $(H_2Se)_2$.

the total deformation energy for the studied dimers. We notice that the value of $E_{\text{int}}^{\mathcal{G}\cdots\mathcal{H}}$ with the largest magnitude corresponds, as expected, to the water dimer. More interesting is the fact that the interaction energy for the other two clusters are very similar (within 1 kcal mol^{-1} of difference). This result further increases the similarities between $(H_2S)_2$ and $(H_2Se)_2$. Moreover, the dissection of the interaction energy afforded by the IQA analyses helps us to understand more thoroughly the intermolecular interactions in these clusters. For example, the IQA classical contribution in $(H_2S)_2$ and $(H_2Se)_2$ is noticeably small (around 1 kcal mol^{-1}). Therefore, all the interaction energy in these dimers comes virtually from the exchange-correlation term. These observations are in sharp contrast with those for $(H_2O)_2$ in which $E_{\text{class}}^{\mathcal{G}\cdots\mathcal{H}}$ has an important contribution to $E_{\text{int}}^{\mathcal{G}\cdots\mathcal{H}}$. The fact that $E_{\text{class}}^{\mathcal{G}\cdots\mathcal{H}}$ has such a small contribution in the formation energy of $(H_2S)_2$ and $(H_2Se)_2$ is opposed to the traditional view that hydrogen bonds are non-covalent interactions in which electrostatics play a non-negligible role. [66, 67]

At this point we consider important to notice that the almost negligible role of electrostatics in the intermolecular contact in $(H_2S)_2$ and $(H_2Se)_2$, is in contradiction with one important criterion of IUPAC concerning the nature of the interaction in HBs, which states that *"The forces involved in the formation of a (H$\cdots$Y) H-bond include those of an electrostatic origin, those arising from charge transfer between the donor and acceptor leading to partial covalent bond formation between H and Y, and those originating from dispersion."* [10][2] We interpret the word *"involved"* in this recommendation of IUPAC to imply a significant role in the interaction as opposed to understand it as a non-zero contribution to the energetics of the molecular contact. Virtually all interactions in chemistry have different from zero contributions from electrostatics, charge transfer, covalency and dispersion. Thus, if we consider that *"involved"* conveys merely non-zero components, then

[2]The diversity of the components of H-bond interactions are also highlighted by Scheiner when he wrote *"All of these distributions of electron density fall under various rubrics such as charge transfer, polarization orbital interactions and induction"*[68] We point out nonetheless that many interactions which are not H-bond will fall into one or more of these categories. This condition contributes to the usual leniency in the characterisation of an interaction as an H-bond.

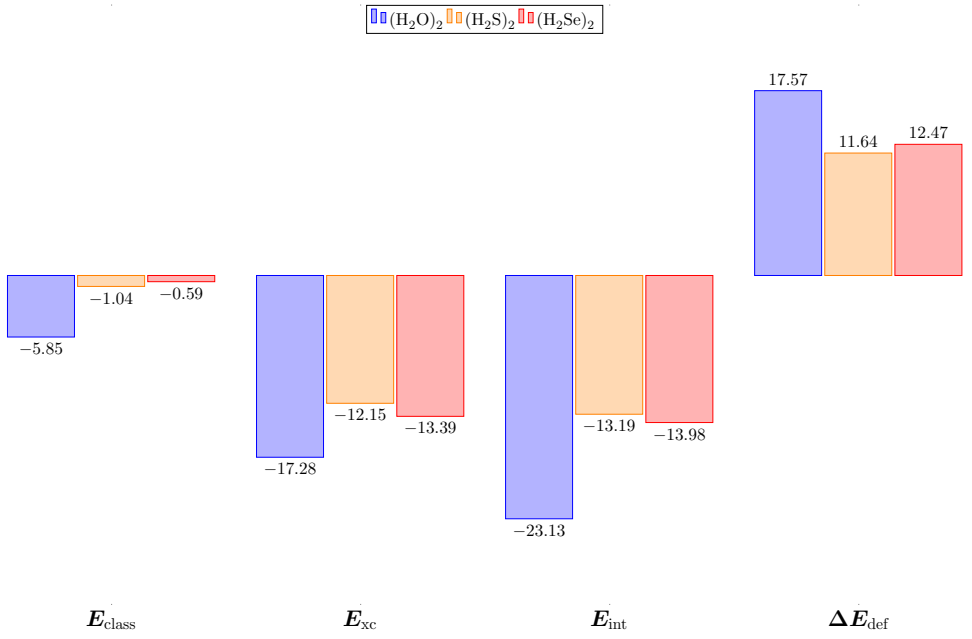

Figure 7: IQA interaction energy ($E_{\text{int}}^{\mathcal{G}\cdots\mathcal{H}}$) and its electrostatic ($E_{\text{class}}^{\mathcal{G}\cdots\mathcal{H}}$) and exchange-correlation ($E_{\text{xc}}^{\mathcal{G}\cdots\mathcal{H}}$) components and the sum of deformation energies ($\Delta E_{\text{def}}^{\mathcal{G}} + \Delta E_{\text{def}}^{\mathcal{H}}$), shown in blue, orange and red respectively, for $(H_2O)_2$, $(H_2S)_2$ and $(H_2Se)_2$. The data are reported in kcal mol^{-1}.

practically every interaction between two electronic systems would fulfill the above-mentioned specification of IUPAC to be considered as an H-bond.

This difference in the electrostatic terms of the intermolecular interaction energy is in good agreement with the fact that the lone pair in the chalcogen atoms within the H-acceptor molecule in $(H_2S)_2$ and $(H_2Se)_2$ does not point to the H-atom in the donor molecule in their equilibrium dispositions (Figures 5(f) and 5(i)). This observation is to be contrasted with the more directional interaction in the $(H_2O)_2$ cluster, as previously discussed. The relative magnitudes of $E_{\text{class}}^{\mathcal{G}\cdots\mathcal{H}}$ for $(H_2O)_2$, on one hand, and $(H_2S)_2$ and (H_2Se) on the other, are consistent with the dipole moment that each molecule has within the dimers. While water molecules, both HB acceptor and HB donor, present relatively large dipole moments, those corresponding to the other two clusters are comparatively small, as schematised in Figure 8. This difference in the magnitude of the dipole moments within the examined dimers is also consistent with the more marked anisotropy of $(H_2O)_2$ with respect to $(H_2S)_2$ and (H_2Se).

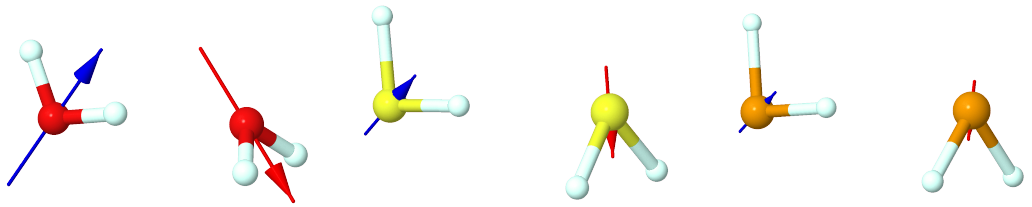

(a) (b) (c)

Figure 8: Graphical representation of the calculated dipole moment for each molecule within the (a) $(H_2O)_2$, (b) $(H_2S)_2$, and (c) $(H_2Se)_2$ clusters in their equilibrium configuration.

The smallness of $E_{\text{class}}^{\mathcal{G}\cdots\mathcal{H}}$ for $(H_2S)_2$ and $(H_2Se)_2$ is also consistent with our analyses of the electrostatic potential. Figure 9 shows the values of this scalar field mapped onto a density isosurface for the studied clusters. The regions with the most negative electrostatic potential in the H-acceptor chalcogen are more sizeable in $(H_2O)_2$ than they are in $(H_2S)_2$ and $(H_2Se)_2$. These areas are barely visible for $(H_2S)_2$ and $(H_2Se)_2$, an indication of an unimportant concentration of charge in the H-acceptor atom in these systems. As a matter of fact, we also observe that the H-acceptor sulphur and selenium atoms have zones of positive electrostatic potential around them. Moreover, these areas are directed to the intermolecular region reducing thereby the magnitude of $E_{\text{class}}^{\mathcal{G}\cdots\mathcal{H}}$ as opposed to what it is observed in $(H_2O)_2$ [69].

The SAPT partition of the formation energy of molecular clusters yields a somewhat different, although compatible perspective to that offered by IQA. Figure 10 shows the different SAPT contributions, *i.e.*, electrostatic (E_{elst}), exchange (E_{exch}), induction (E_{ind}), and dispersion (E_{disp}) [53] to E_{form} in $(H_2O)_2$, $(H_2S)_2$ and $(H_2Se)_2$. Data up to the SAPT2+3 level are shown in the Esi. Table 2 reports the IQA and SAPT components of the equilibrium structures of $(H_2O)_2$, $(H_2S)_2$ and $(H_2Se)_2$. As shown in earlier comparisons [70], SAPT tends to provide larger electrostatic terms due to charge interpenetration which is forbidden in IQA. Moreover, all induction contributions are truly electrostatic in the relaxed IQA densities, hence it is the sum of E_{elst} and E_{ind} that should be compared to the E_{class} component in IQA. In a similar manner, dispersion is a correlation effect, so that E_{disp} is contained in the IQA E_{xc} contribution (see the Theoretical framework section) while the IQA deformation energy of the fragments also includes

Table 2: Comparison between the IQA and SAPT partitions for the formation energy of $(H_2O)_2$, $(H_2S)_2$ and $(H_2Se)_2$. The quantity XR is defined as XR = $E_{def} + E_{xc}$ The data are reported in kcal/mol.

	$(H_2O)_2$		
E_{xc}	−17.28	E_{exch}	7.18
E_{class}	−5.85	E_{elst}	−8.51
E_{def}	17.57	E_{ind}	−2.27
XR	0.29	E_{disp}	−1.85
	$(H_2S)_2$		
E_{xc}	−12.15	E_{exch}	4.28
E_{class}	−1.04	E_{elst}	−2.98
E_{def}	11.64	E_{ind}	−1.09
XR	−0.51	E_{disp}	−1.90
	$(H_2Se)_2$		
E_{xc}	−13.39	E_{exch}	4.99
E_{class}	−0.59	E_{elst}	−2.98
E_{def}	12.47	E_{ind}	−1.14
XR	−0.92	E_{disp}	−2.20

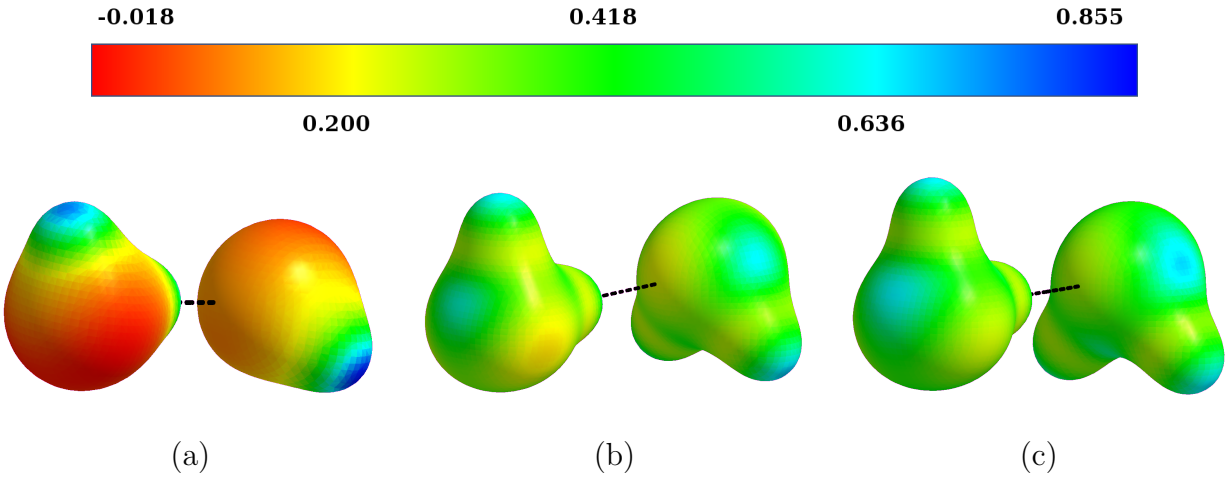

Figure 9: Total electrostatic potential mapped onto a density isosurface $\rho(\mathbf{r}) = 0.03$ a.u. for the dimers of chalcogen hydrides examined herein. The maximum and minimum values are 0.646 and -0.050 a.u.; 0.490 and 0.092 a.u.; and 0.500 and 0.132 a.u. for (a) $(H_2O)_2$, (b) $(H_2S)_2$, and (c) $(H_2Se)_2$ respectively.

excitations of the fragments to charged resonance structures which are not present in the frozen SAPT moieties. Finally, the attractive contribution coming from covalency is added in IQA to the E_{xc} term, and it is absent in SAPT. Taking the water dimer as an example, this means that E_{xc} includes the effects of covalency which are not described by SAPT. These considerations lead to a fruitful comparison between the IQA and SAPT results. In a standard H-bonded system like $(H_2O)_2$, IQA provides $E_{\text{xc}} + \Delta E_{\text{def}} \gtrsim 0$ [71], and $E_{\text{elst}} + E_{\text{ind}} + E_{\text{exch}} < 0$ in SAPT. On the contrary, in both $(H_2S)_2$ and $(H_2Se)_2$, $E_{\text{xc}} + \Delta E_{\text{def}} < 0$, while $E_{\text{elst}} + E_{\text{ind}} + E_{\text{exch}} > 0$ in SAPT. In IQA, covalency and dispersion effects are predominant in $(H_2S)_2$ and $(H_2Se)_2$. In SAPT parlance, dispersion alone can explain the binding energy of the dimers, although the magnitude of E_{disp} is similar in the three dimers. The view coming from perturbation theory is thus in line with interpreting the two heavier dimers as van der Waals complexes. Here we stress that this image completely misses the interfragment electron exchange uncovered by IQA. Anyway, in both partitions, $(H_2O)_2$ behaves differently to its heavier counterparts.

We would like to point out here that when too lenient criterion for the occurrence of an H-bond are used, the qualitative categorisation loses its usefulness. For instance the existence of an intermolecular bond critical point and a corresponding bond path for the XH···Y interaction

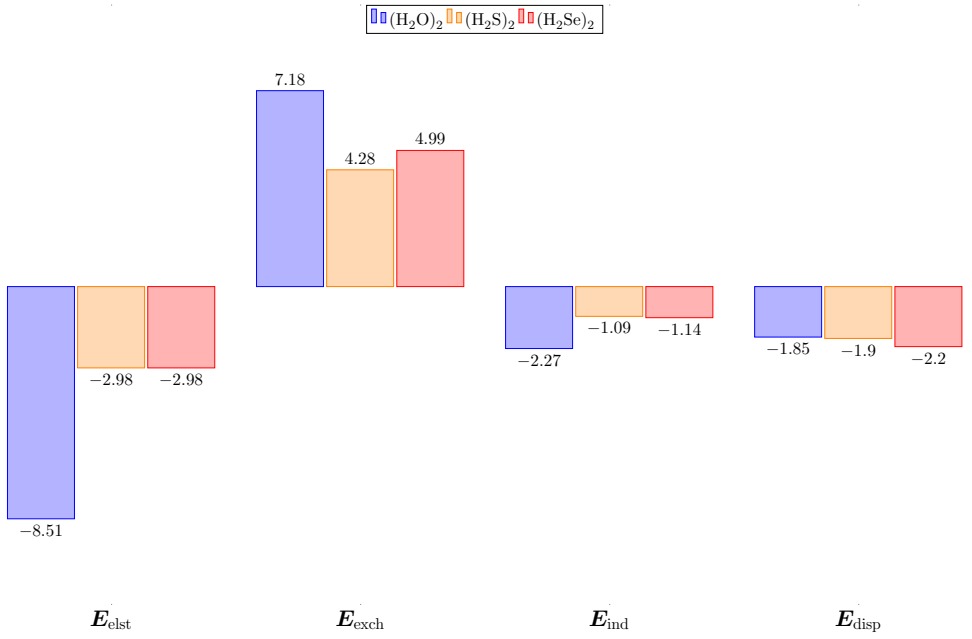

Figure 10: SAPT interaction energy splitting into its electrostatic and induction ($E_{\text{elect+induc}}$), exchange (E_{X}) and dispersion (E_{disp}) terms shown in blue, orange and red respectively, for $(H_2O)_2$, $(H_2S)_2$ and $(H_2Se)_2$. The data are reported in kcal mol^{-1}.

depends of the geometry arrangement of the atoms, as predicated by the Poincaré-Hopf Rule (PHR). [40] Hence, statements such as *"Both Ar···HF and Ne···HF have bond critical points between Ar/Ne and hydrogen and there is a bond path which connects the hydrogen to the rare gas atom"* [54] cannot be used as an indication of hydrogen bonding because such critical points of the electron density will appear for any kind of intermolecular contact: H-bond, van der Waals, hydrophobic, etc. as a consequence of the PHR rule. See for example the molecular graphs in reference [72] for the methane dimer. Yet, $(CH_4)_2$ is not understood as a hydrogen-bonded system. Another example of a criteria which is too lax is the value of the electron density at the corresponding intermolecular bond critical point. Popelier and Koch [73] indicated that BCPs associated at HBs were found in the interval 0.002–0.034. The corresponding values of $\varrho(\mathbf{r})$ at the intermolecular BCPs of several $(CH_4)_2$ configurations fall within this interval of electron densities. [72] Yet, again, $(CH_4)_2$ is not considered as a hydrogen-bonded system. Hereof, one can also find too wide definitions of H-bond based only on either the existence of

a chemical bond, like in the book of Pimentel and McClellan: *"A hydrogen bond is said to exist when (1) there is evidence of a bond and (2) there is evidence that this bond specifically involves a hydrogen bond atom already bonded to another atom"* [74] or even in equilibrium geometries, *"Optimized geometries of $(H_2O)_2$ and $(H_2S)_2$ calculated ab initio are similar and both are hydrogen-bonded."* [75] Following both criteria one should consider $(CH_4)_2$ as 'hydrogen-bonded', which is not the case. Yet, another example of too tolerant statements about H-bond interactions is that *"there is fundamentally no difference between 'charge transfer' and 'hydrogen-bond interactions"*. There are certainly fundamental differences between charge transfer and hydrogen bond interactions. Charge transfer understood as a process occurring in real space involving different atoms or functional groups [3] is a one-directional removal of electron density, as in the LiF crystal, completely decoupled from electron exchange, viz., covalency and for which electron correlation effects such as dispersion are irrelevant. The role of covalency and dispersion can hardly be ignored in the description of H-bonds. Thus, this investigation illustrates that thorough research is required to assess the nature of the intermolecular interaction of borderline cases such as $(H_2S)_2$ and $(H_2Se)_2$. There are other criteria for the characterization of H-bonds that are applicable for any kind of interaction irrespective of its nature. Goswami and Arunan point out that when the barrier for the dissociation of H-bonds is smaller than the zero point energy then the system is not hydrogen bonded. For example, the interaction between the argon dimer and H_2S is not an HB (not even at 0 K) because of this circumstance. Nevertheless, this condition is true for any kind of interaction regardless whether it is an H-bond or not, and therefore it is not useful to distinguish an HB from other type of contacts. Indeed, the H_2S dimer is an experimentally observed cluster identified in a rotational spectrum as opposed to free H_2S units.

Altogether, the electronic structure and quantum chemical topology calculations as well as the electronic energy partitions presented in this investigation indicate that although there is evidence of attractive interactions between the molecules in all the studied clusters, there are

[3] This idea is different to those from orbital-space analyses such as NBO.

also important qualitative differences in the nature of $(H_2O)_2$, on one hand, and $(H_2S)_2$ and $(H_2Se)_2$, on the other. The X···H (X = O, S, Se) distances along with the examination of cooperative effects indicate H-bond interactions in the examined clusters. On the other hand, X···X distances, potential energy curves, the ELF as well as the IQA and SAPT energy partitions suggest a distinctive character of the H-bond in $(H_2O)_2$ with respect to the interactions in $(H_2S)_2$ and $(H_2Se)_2$. We conclude therefore that the intermolecular interactions in $(H_2S)_2$ and $(H_2Se)_2$ are not hydrogen bonds.

Conclusions

We have presented an investigation on the nature of the intermolecular bonding in the $(H_2O)_2$, $(H_2S)_2$ and $(H_2Se)_2$ clusters using correlated electronic structure calculations, quantum chemical topology analyses and electronic energies partitions. While some results indicate that $(H_2S)_2$ and $(H_2Se)_2$ are hydrogen-bonded systems, other point to stark differences in the intermolecular bonding situation between (i) $(H_2O)_2$ on the one hand, and (ii) $(H_2S)_2$ and $(H_2Se)_2$ on the other. For example, the IQA interaction energy for the water dimer includes classical and covalent contributions while for the sulphur and selenium analogues, the interaction is completely dominated by the exchange-correlation term. We also found that $(H_2O)_2$ has a considerably more anisotropic interaction than $(H_2S)_2$ and $(H_2Se)_2$. We came to the conclusion that the H_2S and H_2Se dimers are not hydrogen-bonded clusters. Overall, we expect that the analysis put forward in this work illustrates how the classification of intermolecular interactions (not only hydrogen bonds) in borderline cases requires a thorough investigation of such systems.

Acknowledgements

We gratefully acknowledge financial support from CONACyT/Mexico (grant 253776 and PhD scholarship 436154 for AFA), PAPIIT/UNAM (project IN205118), the Spanish MICINN (grant PGC2018-095953-B-I00), the Principado de Asturias Goverment (grant IDI/2018/000177) and The European Union FEDER funds. We are also grateful to DGTIC/UNAM (project LANCAD-

UNAM-DGTIC-250) for computer time. We also thank the reviewers of the previous version of this work for their criticism which helped considerably to enrich the discussion of this paper.

References

References

[1] T. Steiner, *Angew. Chem. Int. Ed.* **2002**, *41*, 48–76.

[2] G. R. Desiraju, *Acc. Chem. Res.* **2002**, *35*, 565–573.

[3] M. S. Weiss, M. Brandl, J. Sühnel, D. Pal, R. Hilgenfeld, *Trends Biochem. Sci.* **2001**, *26*, 521–523.

[4] T. F. A. de Greef, E. W. Meijer, *Nature* **2008**, *453*, 171–173.

[5] J. D. Smith, *Science* **2004**, *306*, 851–853.

[6] O. O. Brovarets', Y. P. Yurenko, D. M. Hovorun, *J. Biomol. Struct. Dyn.* **2014**, *33*, 1624–1652.

[7] E. Romero-Montalvo, J. M. Guevara-Vela, W. E. Vallejo Narváez, A. Costales, Á. Martín Pendás, M. Hernández-Rodríguez, T. Rocha-Rinza, *Chem. Commun.* **2017**, *53*, 3516–3519.

[8] G. N. Pairas, P. G. Tsoungas, *ChemistrySelect* **2016**, *1*, 4520–4532.

[9] T. S. Moore, T. F. Winmill, *J. Chem. Soc., Trans.* **1912**, *101*, 1635–1676.

[10] E. Arunan, G. R. Desiraju, R. A. Klein, J. Sadlej, S. Scheiner, I. Alkorta, D. C. Clary, R. H. Crabtree, J. J. Dannenberg, P. Hobza, H. G. Kjaergaard, A. C. Legon, B. Mennucci, D. J. Nesbitt, *Pure Appl. Chem.* **2011**, *83*, 1637.

[11] M. Saggu, N. M. Levinson, S. G. Boxer, *J. Am. Chem. Soc.* **2012**, *134*, 18986–18997.

[12] S. J. Grabowski, *J. Phys. Chem. A* **2001**, *105*, 10739–10746.

[13] H. Benedict, I. G. Shenderovich, O. L. Malkina, V. G. Malkin, G. S. Denisov, N. S. Golubev, H.-H. Limbach, *J. Am. Chem. Soc.* **2000**, *122*, 1979–1988.

[14] A. Das, P. K. Mandal, F. J. Lovas, C. Medcraft, N. R. Walker, E. Arunan, *Angew. Chem. Int. Ed.* **2018**, *57*, 15199–15203.

[15] J. S. Loveday, R. J. Nelmes, S. Klotz, J. M. Besson, G. Hamel, *Phys. Rev. Lett.* **2000**, *85*, 1024–1027.

[16] J. K. Cockcroft, A. N. Fitch, *Z. Kristallogr. Cryst. Mater.* **1990**, *193*, 1–19.

[17] J. B. Neaton, N. W. Ashcroft, *Nature* **1999**, *400*, 141–144.

[18] W. J. Evans, M. J. Lipp, C.-S. Yoo, H. Cynn, J. L. Herberg, R. S. Maxwell, M. F. Nicol, *Chem. Mater.* **2006**, *18*, 2520–2531.

[19] M. J. Lipp, W. J. Evans, B. J. Baer, C.-S. Yoo, *Nat. Mater.* **2005**, *4*, 211–215.

[20] Y. Ma, A. R. Oganov, Z. Li, Y. Xie, J. Kotakoski, *Phys. Rev. Lett.* **2009**, *102*, 065501.

[21] P. L. A. Popelier in *Intermolecular Forces and Clusters I*, Springer Berlin Heidelberg, **2005**.

[22] P. L. A. Popelier, *Applications of Topological Methods in Molecular Chemistry*, Springer International Publishing, **2016**.

[23] Z. Badri, C. Foroutan-Nejad, J. Kozelka, R. Marek, *Phys. Chem. Chem. Phys.* **2015**, *17*, 26183–26190.

[24] C. Foroutan-Nejad, Z. Badri, R. Marek, *Phys. Chem. Chem. Phys.* **2015**, *17*, 30670–30679.

[25] J. L. McDonagh, M. A. Vincent, P. L. Popelier, *Chem. Phys. Lett.* **2016**, *662*, 228–234.

[26] J. L. Casalz-Sainz, J. M. Guevara-Vela, E. Francisco, T. Rocha-Rinza, Á. Martín Pendás, *ChemPhysChem* **2017**, *18*, 3553–3561.

[27] K. Eskandari, M. Lesani, *Chem. Eur. J.* **2015**, *21*, 4739–4746.

[28] J. M. Guevara-Vela, D. Ochoa-Resendiz, A. Costales, R. Hernández-Lamoneda, Á. Martín Pendás, *ChemPhysChem* **2018**, *19*, 2512–2517.

[29] O. Brea, O. Mó, M. Yáñez, I. Alkorta, J. Elguero, *Chem. Eur. J.* **2015**, *21*, 12676–12682.

[30] G. Moreno-Alcántar, J. M. Guevara-Vela, R. Delgadillo-Ruíz, T. Rocha-Rinza, Á. Martín Pendás, M. Flores-Álamo, H. Torrens, *New J. Chem.* **2017**, *41*, 10537–10541.

[31] P. I. Dem'yanov, P. M. Polestshuk, V. V. Kostin, *Chem. Eur. J.* **2017**, *23*, 3257–3261.

[32] F. Fuster, S. J. Grabowski, *J. Phys. Chem. A* **2011**, *115*, 10078–10086.

[33] J. R. Lane, J. Contreras-García, J.-P. Piquemal, B. J. Miller, H. G. Kjaergaard, *J. Chem. Theory Comput.* **2013**, *9*, 3263–3266.

[34] J. M. Guevara-Vela, E. Romero-Montalvo, A. Costales, Á. Martín Pendás, T. Rocha-Rinza, *Phys. Chem. Chem. Phys.* **2016**, *18*, 26383–26390.

[35] J. M. Guevara-Vela, E. Romero-Montalvo, A. del Río Lima, Á. Martín Pendás, M. Hernández-Rodríguez, T. Rocha Rinza, *Chem. Eur. J.* **2017**, *23*, 16605–16611.

[36] J. M. Guevara-Vela, E. Romero-Montalvo, V. A. Mora-Gómez, R. Chávez-Calvillo, M. García-Revilla, E. Francisco, Á. Martín Pendás, T. Rocha-Rinza, *Phys. Chem. Chem. Phys.* **2016**, *18*, 19557–19566.

[37] E. Romero-Montalvo, J. M. Guevara-Vela, A. Costales, Á. Martín Pendás, T. Rocha-Rinza, *Phys. Chem. Chem. Phys.* **2017**, *19*, 97–107.

[38] A. Fernández-Alarcón, J. L. Casals-Sainz, J. M. Guevara-Vela, A. Costales, E. Francisco, Á. Martín Pendás, T. Rocha-Rinza, *Phys. Chem. Chem. Phys.* **2019**, *21*, 13428–13439.

[39] A. Fernández-Alarcón, J. M. Guevara-Vela, J. L. Casals-Sainz, A. Costales, E. Francisco, Á. Martín Pendás, T. Rocha Rinza, *Chem. Eur. J.* **2020**, *26*, 17035–17045.

[40] R. F. W. Bader, *Atoms in Molecules. A Quantum Theory*, Oxford University Press, Oxford, **1995**.

[41] X. Fradera, M. A. Austen, R. F. W. Bader, *J. Phys. Chem. A* **1999**, *103*, 304–314.

[42] R. F. W. Bader, *Chem. Rev.* **1991**, *91*, 893–928.

[43] M. A. Blanco, A. Martín Pendás, E. Francisco, *J. Chem. Theory Comput.* **2005**, *1*, 1096–1109.

[44] Á. Martín Pendás, J. L. Casals-Sainz, E. Francisco, *Chem. Eur. J.* **2018**, *25*, 309–314.

[45] J. L. Casals-Sainz, J. M. Guevara-Vela, E. Francisco, T. Rocha-Rinza, Á. Martín Pendás, *ChemPhysChem* **2017**, *18*, 3553–3561.

[46] J.-Q. Wang, S. Stegmaier, T. Fässler, *Angew. Chem. Int. Ed.* **2009**, *48*, 1998–2002.

[47] Y. Feng, L. Cheng, *RSC Advances* **2015**, *5*, 62543–62550.

[48] A. D. Becke, K. E. Edgecombe, *J. Chem. Phys.* **1990**, *92*, 5397–5403.

[49] B. Silvi, A. Savin, *Nature* **1994**, *371*, 683–686.

[50] A. Savin, R. Nesper, S. Wengert, T. F. Fässler, *Angew. Chem. Int. Ed.* **1997**, *36*, 1808–1832.

[51] E. R. Johnson, S. Keinan, P. Mori-Sánchez, J. Contreras-García, A. J. Cohen, W. Yang, *J. Am. Chem. Soc.* **2010**, *132*, 6498–6506.

[52] M. Alonso, T. Woller, F. J. Martín-Martínez, J. Contreras-García, P. Geerlings, F. De Proft, *Chem. Eur. J.* **2014**, *20*, 4931–4941.

[53] B. Jeziorski, R. Moszynski, K. Szalewicz, *Chemical Reviews* **1994**, *94*, 1887–1930.

[54] M. Goswami, E. Arunan, *Phys. Chem. Chem. Phys.* **2009**, *11*, 8974–8983.

[55] S. Sarkar, M. Monu, B. Bandyopadhyay, *Phys. Chem. Chem. Phys.* **2019**, *21*, 25439–25448.

[56] F.-M. Tao, W. Klemperer, *J. Chem. Phys.* **1995**, *103*, 950–956.

[57] V. F. Lotrich, H. L. Williams, K. Szalewicz, B. Jeziorski, R. Moszynski, P. E. S. Wormer, A. van der Avoird, *J. Chem. Phys.* **1995**, *103*, 6076–6092.

[58] G. Chałasiński, M. M. Szczęśniak, S. Scheiner, *J. Chem. Phys.* **1991**, *94*, 2807–2816.

[59] S. Tsuzuki, K. Honda, T. Uchimaru, M. Mikami, A. Fujii, *J. Phys. Chem. A* **2006**, *110*, 10163–10168.

[60] M. García-Revilla, T. Rocha-Rinza, *Curr. Org. Chem.* **2011**, *15*, 3627–3651.

[61] A. Savin, B. Silvi, F. Colonna, *Can. J. Chem.* **1996**, *74*, 1088–1096.

[62] R. Taylor, O. Kennard, W. Versichel, *J. Am. Chem. Soc.* **1983**, *105*, 5761–5766.

[63] F. Fuster, B. Silvi, *Theor. Chem. Acc.* **2000**, *104*, 13–21.

[64] E. Espinosa, E. Molins, C. Lecomte, *Chem. Phys. Lett.* **1998**, *285*, 170 – 173.

[65] Á. Martín Pendás, M. A. Blanco, E. Francisco, *J. Comput. Chem.* **2006**, *28*, 161–184.

[66] A. J. Stone, *The theory of intermolecular forces*, Oxford University Press, Oxford, **2016**.

[67] S. C. C. van der Lubbe, C. Fonseca Guerra, *Chem. Asian J.* **2019**.

[68] S. Scheiner, *J. Chem. Phys.* **2020**, *153*, 140901.

[69] M. H. Kolář, P. Hobza, *Chem. Rev.* **2016**, *116*, 5155–5187.

[70] E. Francisco, A. Martín Pendás, *Non-covalent Interactions in Quantum Chemistry and Physics: Theory and Applications*, Elsevier, **2017**.

[71] Á. Martín Pendás, M. A. Blanco, E. Francisco, *J. Chem. Phys.* **2006**, *125*, 184112.

[72] V. Duarte Alaniz, T. Rocha-Rinza, G. Cuevas, *J. Comput. Chem.* **2015**, *36*, 361–375.

[73] U. Koch, P. L. A. Popelier, *The Journal of Physical Chemistry* **1995**, *99*, 9747–9754.

[74] G. Pimentel, A. McClellan, *The Hydrogen Bond*, Franklin Classics Trade Press, **2018**.

[75] E. Arunan, D. Mani, *Faraday Discuss.* **2015**, *177*, 51–64.